

Figure S1: MLL-*AF4* target gene expression by microarray. Scatter plots comparing the expression of (A) *CDK6* (B) *MYC* (C) *HOXA9* and (D) *MEIS1* from the corresponding normalized fluorescence intensities on the microarray. $n=14$ (ETV/RUNX1); $n=15$ (E2A/PBX1); $n=15$ (MLL). (1-way ANOVA followed by Bonferroni's test, * $P < 0.05$; ** $P < 0.01$; *** $P < 0.001$). Data represent mean \pm SD.

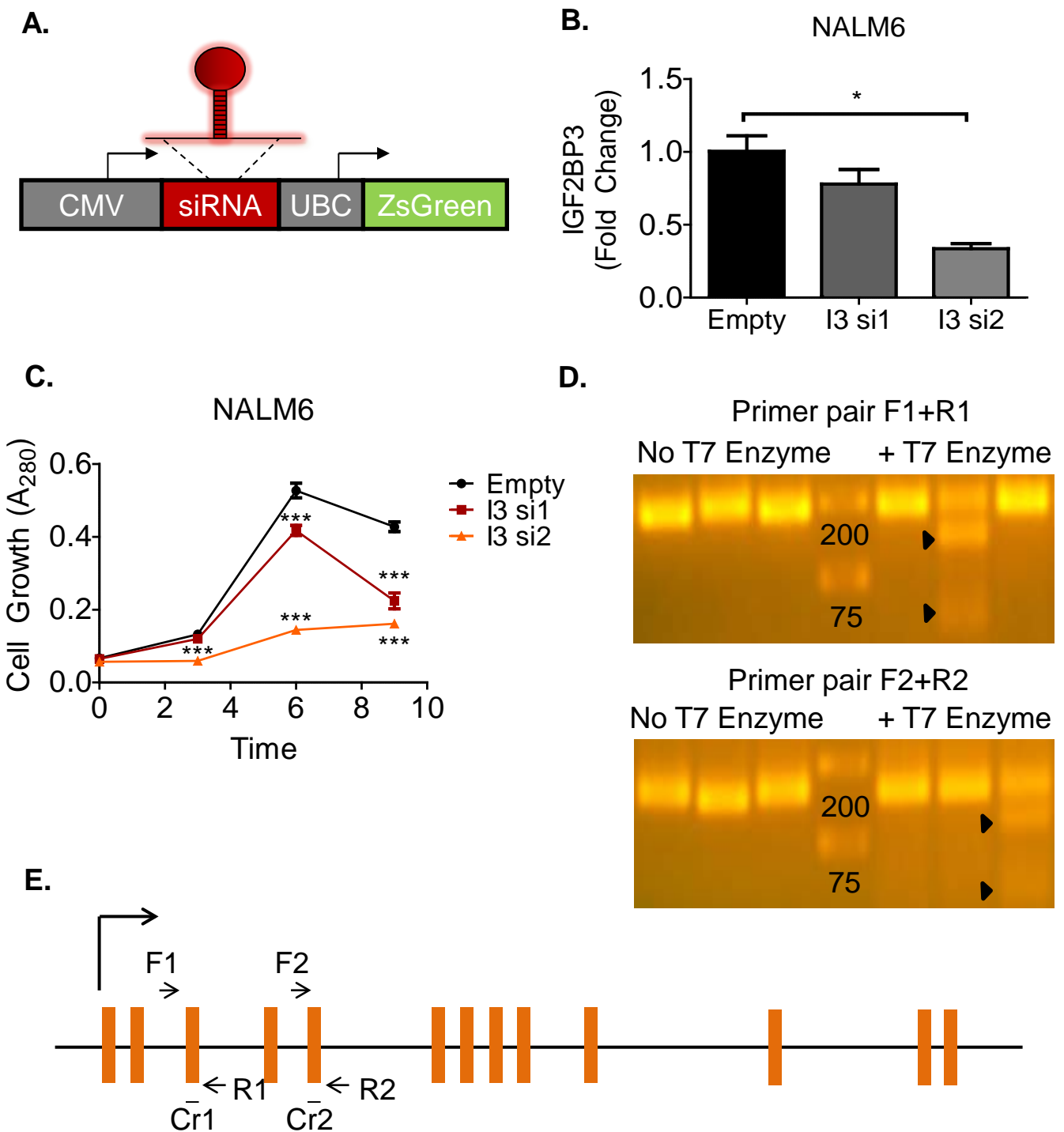


Figure S2: Knockdown of IGF2BP3 in B-ALL cell lines (A) Schematic of the lentiviral vector used for IGF2BP3 knockdown (B) IGF2BP3 knockdown by lentiviruses in NALM6 cell line (t test, $*P < 0.05$) and (C) Reduced cell proliferation (MTS assay) in NALM6 after IGF2BP3 knockdown (t test, $***P < 0.001$ for all comparisons) (D) T7 Endonuclease assay of PCR done using primer pair F1 and R1 (top panel) and DNA extracted from RS4;11 cells stably integrated with LentiCRISPR, Cr1 or Cr2 (Lanes 1-3 and 5-7). On addition of T7 enzyme cleavage, is seen only in the Cr1 integrated cells (arrowheads). Bottom panel shows T7 assay done using the same samples and primer pair F2 and R2. Cleavage is seen only in the Cr2 integrated cells (arrowheads) (E) Human IGF2BP3 gene structure showing the location of exons (in orange) and targets of the CRISPR guide RNAs (Cr1 and Cr2); Primer pairs F1 and R1 flanking the target site of Cr1 as well as primer pairs F2 and R2 flanking the Cr2 target site are also shown. I3, IGF2BP3. Data represent mean \pm SD.

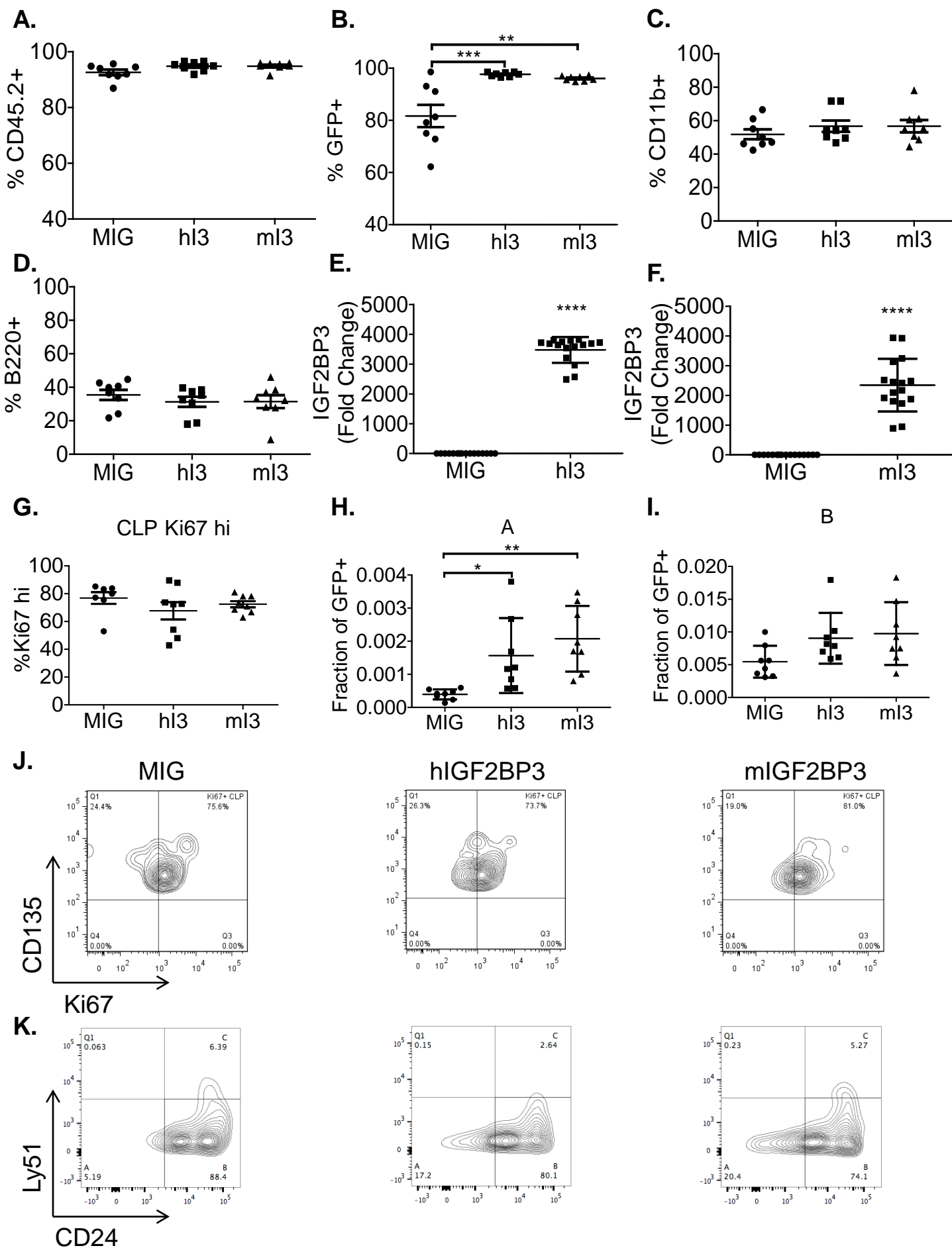


Figure S3: Bone marrow immunophenotypic analyses. Analysis at 24 weeks after IGF2BP3 overexpression shows (A) similar engraftment, (B) increased GFP expressing cells (1-way ANOVA followed by Bonferroni's test, $**P < 0.01$; $***P < 0.001$). and (C) similar numbers of myeloid and (D) B-cells. $n=8$ for all three groups. (E and F) Confirmation of overexpression of human and mouse IGF2BP3 in mouse bone marrow by qPCR (t test, $****P < 0.0001$). Mouse Actin was used as internal control. $n = 16$ for all groups. (G) Ki67 staining of CLPs showing no significant difference and (J) representative FACS plots. (H-I) Increased Hardy fractions A (1-way ANOVA followed by Bonferroni's test, $*P < 0.05$; $**P < 0.01$) and B after IGF2BP3 overexpression with (K) representative plots. $n=8$ for all three groups. hl3, human IGF2BP3; ml3, murine IGF2BP3; CLP, common lymphoid progenitor; BMT, bone marrow transplantation. Three separate BMT experiments were completed for validation. Data represent mean \pm SD.

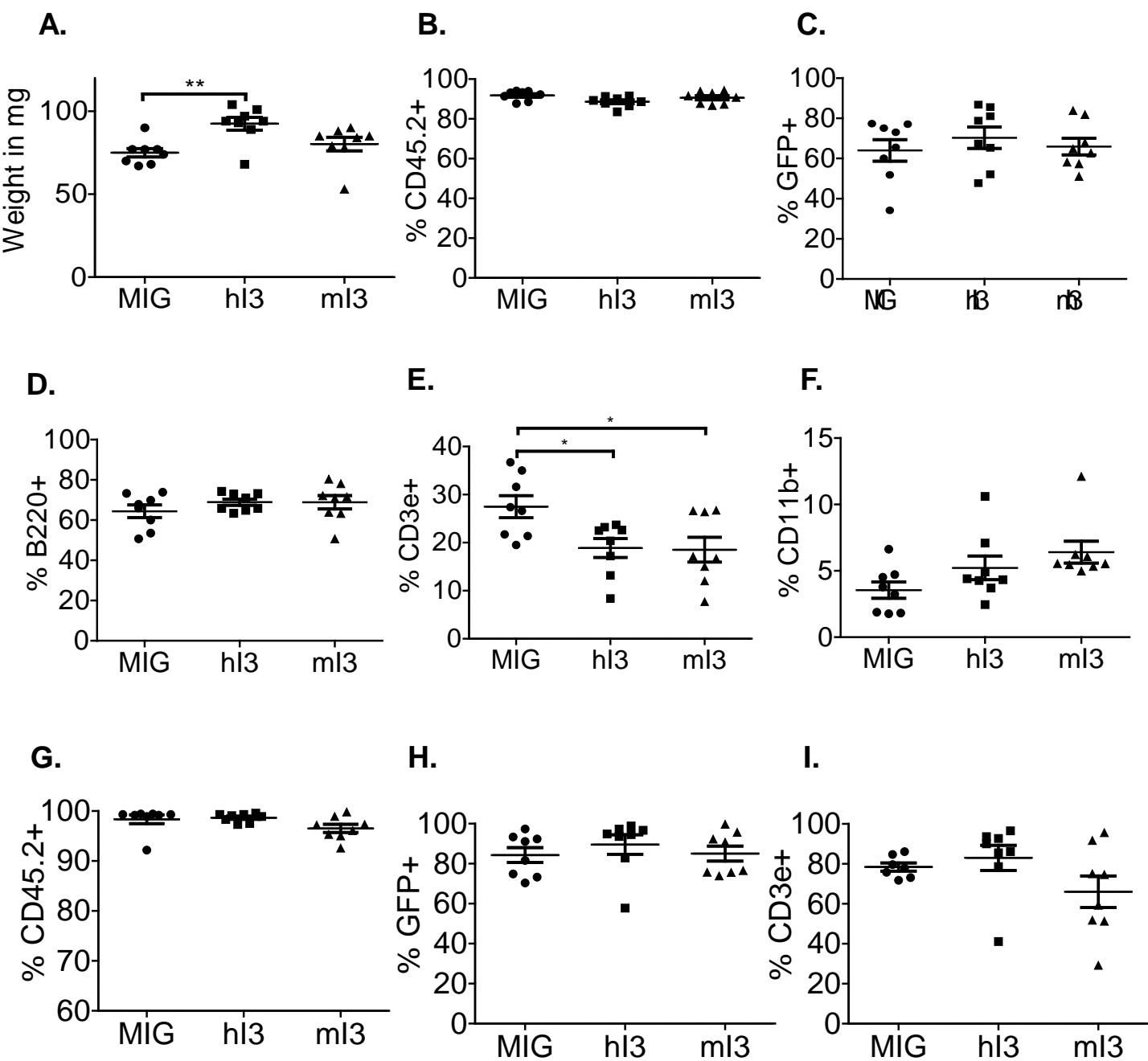


Figure S4: Immunophenotypic analyses of spleen and thymus with enforced expression of IGF2BP3 (A) Spleen analysis at the end of 27 weeks after IGF2BP3 overexpression shows significantly elevated spleen weights (1-way ANOVA followed by Bonferroni's test, $**P < 0.01$), (B) similar engraftment, (C) GFP expressing cells and (D) B-cells. (E) Decreased numbers of T-cells (1-way ANOVA followed by Bonferroni's test, $*P < 0.05$) and (F) elevated myeloid cells are also seen in the spleen (G-I) Enumeration of CD45.2, GFP, and CD3e+ cells, respectively, in thymi from control and human and murine IGF2BP3 overexpressing mice show no statistically significant differences. $n=8$ for all three groups. Three separate BMT experiments were completed for validation. Data represent mean \pm SD.

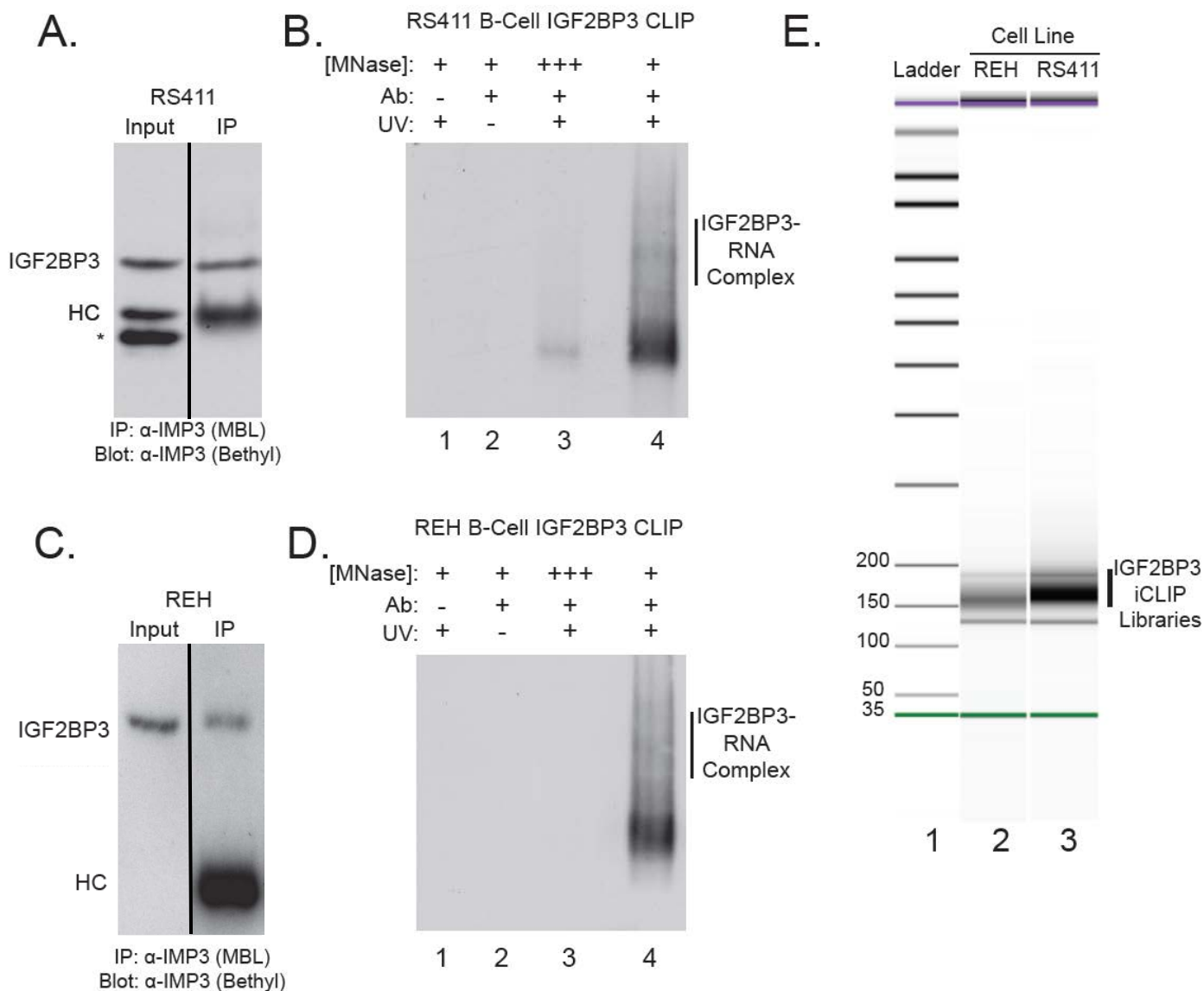


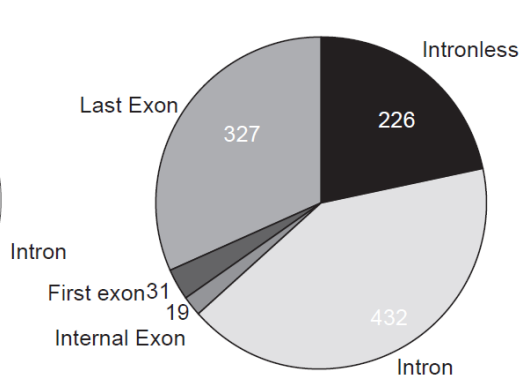
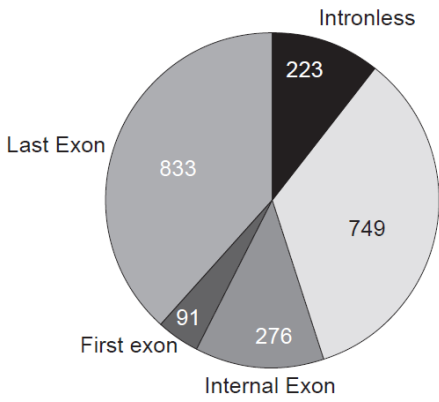
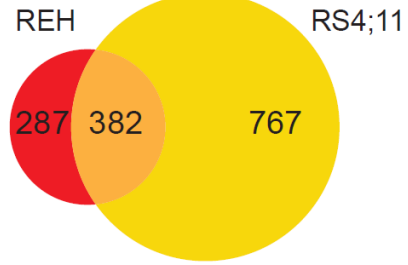
Figure S5: Purification of IGF2BP3-RNA complexes from human leukemia cell lines using crosslinking immunoprecipitation (CLIP). (A) Western blot of RS4;11 whole cell lysate and anti-IGF2BP3 immunoprecipitate. Membrane is probed with anti-IGF2BP3. IgG heavy chain (HC) and a cross-reactive protein (*) are indicated on the blot. (B) Autoradiograph of protein-RNA complexes isolated by CLIP from RS4;11 cells. UV-dependent and nuclease-sensitive IGF2BP3-RNA complexes are indicated. (C and D) As in panels A and B, but using REH cell lysates. (E) Bioanalyzer trace of pooled amplicon libraries from REH and RS4;11 cells (lanes 2 and 3, respectively). Lanes in panels (A) and (C) were run on the same gel but were noncontiguous. IMP3, IGF2BP3; MNase, micrococcal nuclease.

A. RS4;11 cells

B. REH cells

C.

Overlap of Genes targets identified by iCLIP



D. RS4;11 iCLIP Correlations

E. REH iCLIP Correlations

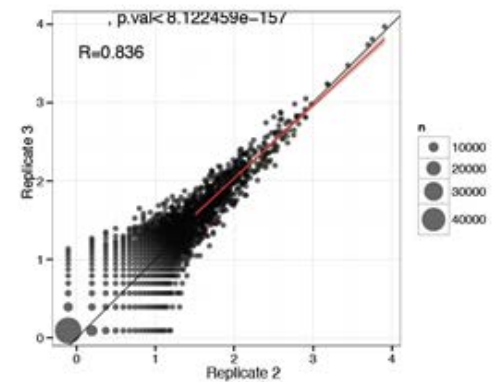
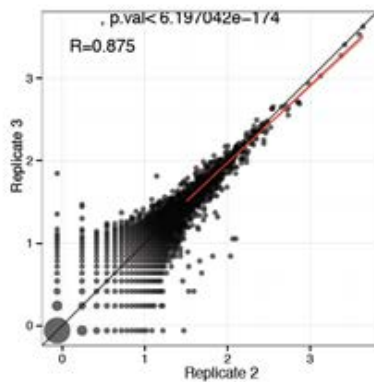
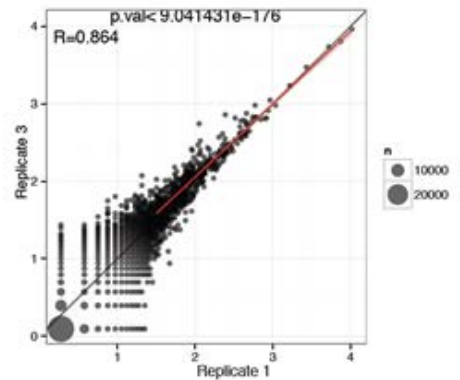
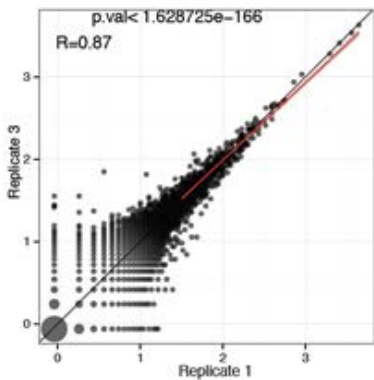
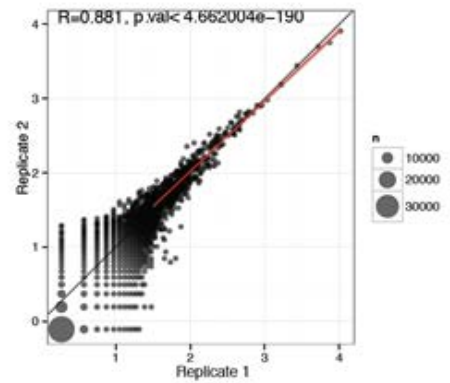
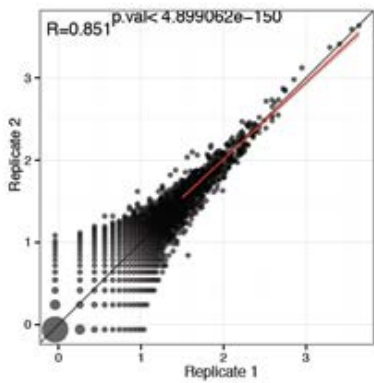


Figure S6: Annotation and overlap of IGF2BP3 binding sites identified in human leukemia cell lines. (A) Annotation of peaks called in RS4;11 cells. (B) Annotation of peaks called in REH cells. (C) Pie charts showing the count of significant CLIP peaks in different regions of protein coding genes. Venn Diagram of genes identified in the iCLIP analysis of IGF2BP3 in REH (red) and RS4;11 cells (Yellow). (D and E) Correlation of replicate IGF2BP3 iCLIP experiments (D) Comparison of iCLIP from RS4;11 cells and (E) REH cells. Spearman's rank correlation coefficient (R) and *P* value are given for each comparison.

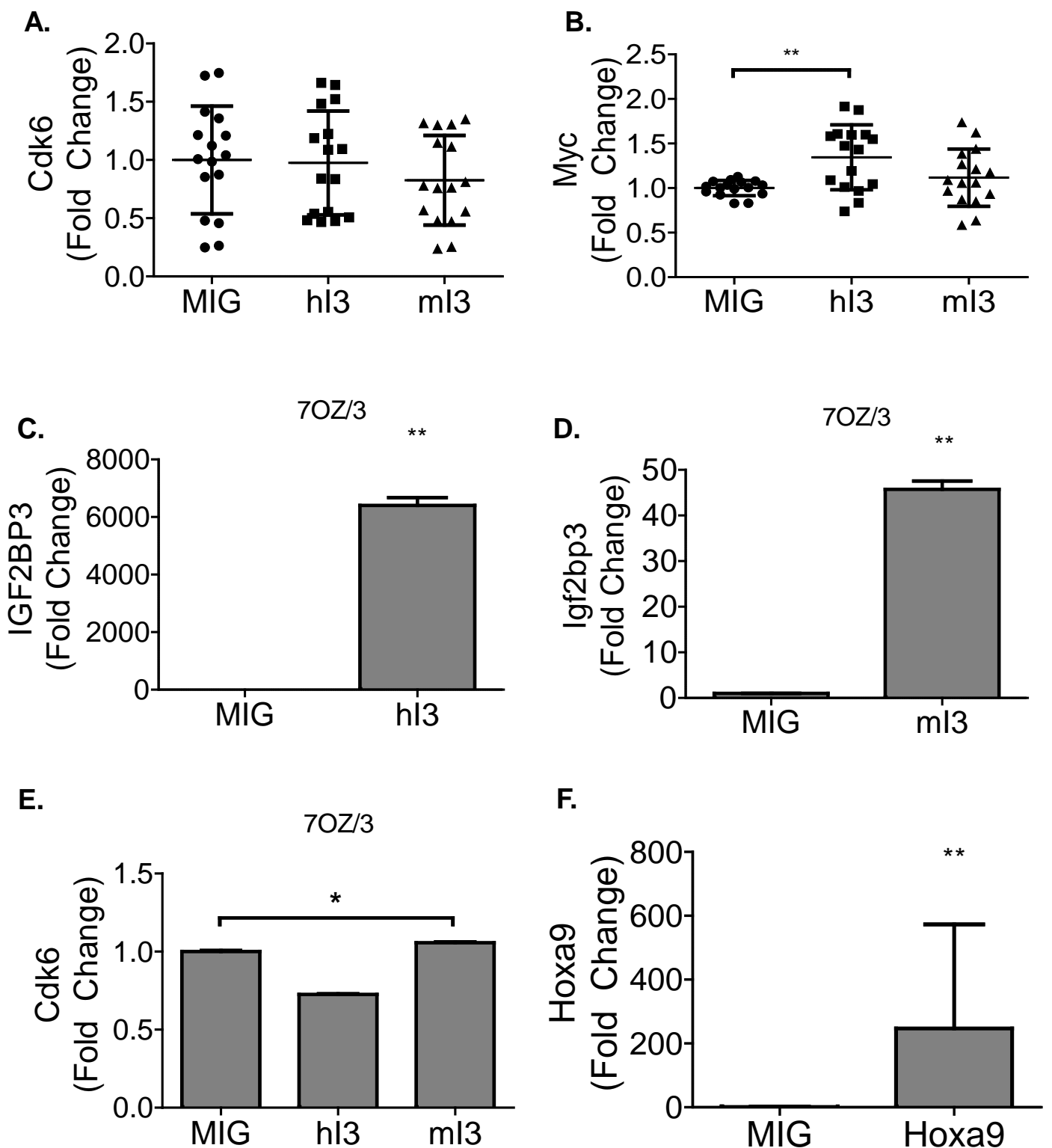


Figure S7: Expression of putative targets of IGF2BP3 (A and B) mRNA expression of Cdk6 and Myc in mouse bone marrow after IGF2BP3 over expression (1-way ANOVA followed by Bonferroni's test, $**P < 0.01$). $n = 16$ for all groups. Three separate BMT experiments were completed for validation. (C) qPCR confirmation of overexpression of hl3 and (D) ml3 in mouse 7OZ/3 cells. (t test, $**P = 0.0018$, $**P = 0.0017$, respectively) (E) qPCR of Cdk6 in 7OZ/3 after IGF2BP3 overexpression (1-way ANOVA followed by Bonferroni's test, $*P < 0.05$). (F) qPCR confirmation of overexpression of Hoxa9 in mouse bone marrow of competitive repopulation study (t test, $**P = 0.0054$). Competitive repopulation study was completed three times for validation. Data represent mean \pm SD.

Table S5: List of primers, siRNAs and CRISPR guide RNAs

Primer	Sequence
Human primers for qPCR	
qhActinF	CATGTACGTTGCTATCCAGGC
qhActinR	CTCCTTAATGTCACGCACGAT
qhL32F	GGAGCGACTGCTACGGAAG
qhL32R	GATACTGTCCAAAAGGCTGGAA
qhIGF2BP3F	CCTGGTGAAGACTGGCTACG
qhIGF2BP3R	ATCCAGCACCTCCCCTGTA
qhCDK6F	GCTGACCAGCAGTACGAATG
qhCDK6R	GCACACATCAAACAACCTGACC
qhCD44F	AGTCACAGACCTGCCCAATG
qhCD44R	AACCTCCTGAAGTGCTGCTC
q-h-POLR2AF	CATCAAGAGAGTCCAGTTCGG
q-h-POLR2AR	CCCTCAGTCGTCTCTGGGTA
MYCF	GCTGCTTAGACGCTGGATTT
MYCR	TAACGTTGAGGGGCATCG
CDK6F	TGATCAACTAGGAAAATCTTGGA
CDK6R	GGCAACATCTCTAGGCCAGT
18s-rRNAF	CTTCCACAGGAGGCCTACAC
18s-rRNAR	CGCAAATATGCTGGAACCTT
Mouse primers for qPCR	
qmL32F	AAG CGA AAC TGG CGG AAA C
qmL32R	TAA CCG ATG TTG GGC ATC AG
qmActin1F	GATCTGGCACCACACCTTCT
qmActin1R	GGGGTGTTGAAGGTCTCAA
qmIGF2BP3F	GGATCGGTGTCCAAGCAGAA
qmIGF2BP3R	GCCTTCAGGGGTAGAGAGGA
qmCdk6F	TCTCACAGAGTAGTGCATCGT
qmCdk6R	CGAGGTAAGGGCCATCTGAAAA
qmMycF	TCT CCA TCC TAT GTT GCG GTC
qmMycR	TCC AAG TAA CTC GGT CAT CAT CT
CRISPR primers for T7 assay	
IMP3Cr1DNAF	TTCTGCAGGATTCGGAAACT
IMP3Cr1DNAR	GCACGGGTCATAGGAGAAGA
IMP3Cr2DNAF	GAACACTGACTCGGAAACTGC
IMP3Cr2DNAR	CACCTACCAGCCCTTCTCAG

siRNA sense strand sequence	
IGF2BP3 si1	AATTCCTGCAATGGAGATATC
IGF2BP3 si2	TTCATGATCTCCTCCTCAGCT
Cloning primers	IGF2BP3, T7 IGF2BP3, KH, RRM into MIG: Between BgIII and XhoI
hIMP3CDS1F	atctgaGGATCCcgagaagacgaggggaacaa
hIMP3CDS1R	atgcagCTCGAGtctgtgtggctgttct
mIMP3CDS1F	atctgaGGATCCtgggtcactgtgtgggttg
mIMP3CDS1R	atgcagCTCGAGtgggttgcatctgcctct
T7IMP3F	agcataAGATCTatggcatcgatgacaggtggc
T7IMP3R	atgcagCTCGAGcaccctgaagttctcaggatc
Cloning primers	CDK6 and MYC 3' UTR into pMirGlo: Between SacI and XhoI unless specified MYC 3' UTR binding site deletions into pMirGlo: Between
CDK6UTR1F	atcgagGAGCTCgaaaacctggattcccacct
CDK6UTR1R	cgttcaCTCGAGAGTGCAGCAACCTCCATTCT
CDK6UTR2FNhe	atcgagGCTAGCGGAGGTTGCTGCACTCAGA
CDK6UTR2R	cgttcaCTCGAGTGGTGGCATATTCACCTTTAACAT
CDK6UTR3F	atcgagGAGCTCTCCAAAAGCAGGCTTTAATTG
CDK6UTR3R	cgttcaCTCGAGCCTAAGTTGTTATGCTCATATACTTCA
CDK6UTR4F	atcgagGAGCTCGCCCTAAAATACCAAAGACCA
CDK6UTR4R	cgttcaCTCGAGTGATAAACACCTAGATACCCAAAA
CDK6UTR5F	atcgagGAGCTCCTAAGCCCCCAAATAAGCTG
CDK6UTR5R	cgttcaCTCGAGAAGACATCCAGTTTCCAAAGGA
mycUTRpMirF	atcgagGAGCTCGGAAAAGTAAGGAAAACGATT
mycUTRpMirR	cgttcaCTCGAGTTTGGCTCAATGATATATTTG
5'MYCUTR-3R	GTAATAATATGTAAGTACTGCTATAAACGTTTTA
3'MYCUTR-3F	AGCAGTTACATATATAGTACCTAGTATTATAG
5'MYCUTR-4R	AATCAACTTTTTAAATAAAAAAATTAGGGT
3'MYCUTR-4F	TTTTATTTAAAAGTTGATTTTTTTCTATTG
Cloning CRISPR guide RNAs	Top and bottom strands to anneal and insert into LentiCRISPR
CrIMP31T	caccgATATCCCGCCTCATTACAG
CrIMP31B	aaacCTGTAAATGAGGCGGGATATc
CrIMP32T	caccgAGCTTGGTCCTTACTGGAAT
CrIMP32B	aaacATTCCAGTAAGGACCAAGCTc

Table S6: List of antibodies used for flow cytometry and gating schematics

Lineage staining	
CD3e (100308)	PE
CD11b (101216)	PE-Cy7
B220 (103236)	PercP-Cy 5.5
CD45.1 (110715)	APC-Cy7
CD45.2 (109813)	APC

Bone marrow HSC/LMPP staining	
CD117 (105826)	APC-Cy7
Sca1 (108123)	PerCP-Cy 5.5
CD135 (17-1351-82)	APC
CD127 (135013)	PE-Cy7
CD150 (115903)	PE
Biotin (100304, 13-0041-82, 100704, 103204, 108703, 116204, 118103, 109203)	CD3e, CD4, CD8, B220, NK1.1, Ter119, TCR beta, TCR gamma-delta
Streptavidin-Pacific Blue (48-4317-82)	
HSC	Lin- CD117 hi Sca1 hi CD150++
LMPP	Lin- CD117 hi Sca1 hi CD135+ CD127-
CLP	Lin- CD117 int Sca1 int CD135+ CD127+
For intracellular staining, CD150-PE was replaced by Ki67-PE(652403), CDK6 (sc-177) with goat anti-rabbit IgG-PE (sc-3739), or MYC-PE (sc-40 PE).	

Bone marrow Hardy staining	
B220 (103236)	PerCP-Cy 5.5
IgM (1020-09S)	PE
CD43 (BDB560663)	APC
CD24 (25-0242-80)	PE-Cy7
Ly51(108303)	APC-Cy7

Hardy Fractions	
A	B220+ IgM- CD43+ CD24- Ly51-
B	B220+ IgM- CD43+ CD24+ Ly51-
C	B220+ IgM- CD43+ CD24+ Ly51+
D	B220+ IgM- CD43-
E and F	B220+ IgM+

All antibodies were procured from Biolegend, ebioscience, Santa Cruz Biotechnology, Southern Biotech, or BD Biosciences. Catalog numbers are listed in parenthesis.